X-ray absorption spectroscopy and CO oxidation activity of Au/Al_2O_3 treated with NaCN

Jason T. Calla and Robert J. Davis*

Department of Chemical Engineering, University of Virginia, Charlottesville, Virginia 22094-4741, USA

Received 10 August 2004; accepted 13 October 2004

Gold nanoparticles were supported on Al_2O_3 by a deposition–precipitation method followed by heating in He. The resulting catalyst was then treated with NaCN solutions to remove most of the gold. X-ray absorption spectroscopy at the Au L_{III} edge was used to monitor the oxidation state and atomic structure of Au throughout the procedure. The gold or a Au/Al_2O_3 sample after deposition–precipitation was in a +3 oxidation state and was subsequently reduced to metal after heating to 623 K in He. Treatment of a reduced sample with either 1 or 2 wt.% NaCN in water removed 79% or 86% of the Au, respectively. Although the remaining Au was cationic, it was also reduced to metal after heating to 623 K in He. The rate of CO oxidation per gold atom, the apparent activation energy, and the orders of reaction were unaffected by the NaCN treatments. These results show that alumina does not stabilize cationic Au species and that metallic Au appears to be important for the CO oxidation reaction. The presence of water or H_2 increased the rate of CO oxidation over all of the Au/Al_2O_3 catalysts. However, the promotional effect of co-fed water was greater over the NaCN treated samples.

KEY WORDS: gold, alumina, carbon monoxide, oxidation, water, hydrogen, carbon dioxide, EXAFS, XANES, sodium cyanide, oxygen.

1. Introduction

Although bulk gold is the noblest of metals [1], supported gold nanoparticles are very active in a variety of catalytic reactions. It was not until Haruta *et al.* [2] demonstrated the ability of gold particles to effectively catalyze the oxidation of CO and H_2 that intense study has been focused on this unusual system. Many explanations for the source of gold's reactivity have been proposed, however, the underlying principles of this phenomenon have been elusive [3]. Indeed, high catalytic activity has been attributed to anionic, metallic, and cationic Au species.

One school of thought proposes that anionic gold is the key feature of an active CO oxidation catalyst. A combination of work on gas-phase, anionic clusters [4], MgO supported Au clusters [5,6], and quantum chemical calculations [4–6] suggests that oxygen vacancy F-center defects at the metal–support interface facilitate electron transfer to the Au metal particle and activate it for catalysis.

Others indicate that metallic Au is necessary for high activity. Haruta and coworkers concluded that Au nanoparticles with strong support interactions are essential for high catalytic activity [7,8]. Several research groups have used density functional theory to explore the barriers to adsorption and reaction of CO and O_2 on different gold surfaces [9,10]. Their results indicate that low-coordinated gold atoms provide energetically favorable sites, allowing a path for CO oxidation that is unfavorable on Au (111). Therefore, the high activity of Au nanoparticles is suggested to be the result of a high concentration of low-coordinated surface atoms. The metal-to-nonmetal transition is also observed with the reduction of gold particle size. Valden *et al.* [11] used scanning tunneling microscopy/spectroscopy and CO oxidation kinetic measurements to study gold particles on a planer TiO_2 substrate. They found that 3.5 nm gold particles were the most active in the reaction and that the metal-to-nonmetal transition also occurred near this particle size. Based on these results, they associated the high activity of Au to a quantum size effect with respect to the metal particle thickness.

High catalytic activity for CO oxidation has also been attributed to the presence of cationic Au. Guzman and Gates [12] observed a mixture of Au^{1+} and Au° on MgO under CO oxidation conditions using *in situ* X-ray absorption spectroscopy (XAS). Hodge *et al.* [13] used ^{197}Au Mössbauer spectroscopy to characterize gold supported on α-Fe_2O_3 and found samples containing the highest concentration of Au^{3+} oxyhydroxide possessed the highest activity for CO oxidation. Bond and Thompson, as well as Kung and co-workers have similarly suggested that the active site is an ensemble of cationic and metallic gold [14–16].

The recent work of Fu *et al.* [17] clearly showed that cationic Au on a CeO_2-based support catalyzes the water–gas shift reaction, while metallic Au plays no role in the reaction. Fu *et al.* first supported Au onto La-doped CeO_2 via a deposition–precipitation method. The sample was then calcined in air at 673 K for 10 h prior to further testing. X-ray photoelectron spectroscopy

*To whom correspondence should be addressed.
E-mail: rjd4f@virginia.edu

1011-372X/05/0100–0021/0

(XPS) identified both cationic and metallic Au present on the sample. A portion of this material was then treated with a 2 wt.% NaCN solution to remove more than 90% of the Au from the sample. Following calcination at 673 K for 2 h, only cationic Au was detected on the sample by XPS. Fu *et al.* found that the rate of the water–gas shift reaction did not scale with Au loading. The original and NaCN treated samples had the same apparent activation energy and rate *per surface area* of catalyst. A NaCN-treated sample exposed to reaction conditions could not be leached further, indicating metallic Au particles were not formed during reaction. Thus, Fu *et al.* concluded that the active oxidation state of this, catalyst for the water–gas shift reaction was cationic Au, probably stabilized at defects in the $Ce(La)O_2$ support, and that any metallic particles formed on the surface were mere spectators in the reaction.

In the current work, a similar NaCN treatment was performed on alumina-supported Au nanoparticles to probe the ability of alumina to stabilize cationic gold. The oxidation state of the Au was followed throughout the process by XAS. The resulting samples were also tested as catalysts in the oxidation of CO, with and without added H_2 or H_2O.

2. Experimental methods

2.1. Catalyst preparation

The catalyst used in this study was prepared by a deposition–precipitation method as previously reported [18]. The details of the catalyst preparation areas follows: 0.26 g of $HAuCl_4$ (Aldrich, 99.9%) was added to 80 mL of distilled, deionized water. The gold solution was heated to 343 K and adjusted to pH = 7 with NaOH (Mallinckrodt, 98.6%). The gold solution was then added to a second flask containing 5 g of Al_2O_3 (Mager Scientific AP-312) suspended in 120 mL of distilled, deionized water also at 343 K. After stirring for 2 h, the solution was removed by suction filtration and the catalyst was re-suspended in 100 mL of distilled, deionized water at 343 K for 20 min. This washing procedure was repeated 3 more times after which the filtered catalyst was dried in air at 310 K for 24 h. For kinetic studies, the catalyst was sieved to a particle size of 100–140 mesh (106–150 μm).

2.2. Treatment with NaCN solution

The catalyst was treated with aqueous solutions of NaCN using a process similar to that reported by Fu *et al.* [17]. Prior to contacting with the NaCN solutions, the original Au/Al_2O_3 catalyst was pretreated in flowing He at 623 K for 4 h. Next, 1 g of the thermally-treated catalyst was added to 10 mL of a 2 wt.% NaCN (Alfa Aesar, >95%) aqueous solution adjusted to pH > 12 with a few drops of a 1 M NaOH solution. This mixture was stirred for 70 min at ambient temperature, and then allowed to settle for 20 min. A large portion of the liquid was removed via pipette and replaced with 15 mL of distilled, deionized H_2O. After stirring for 5 min, the catalyst was recovered by suction filtration. A procedure of re-suspending in H_2O, stirring for 20 min, and filtering was repeated 3 times. After the final filtration, the sample was dried in air at 310 K for 24 h.

A separate 1 g batch of the thermally-pretreated, original catalyst was treated with a 1 wt.% NaCN aqueous solution for 10 min with stirring at ambient temperature and allowed to settle for another 10 min. This treated sample was re-suspended, stirred, and recovered according to the wash procedure described above.

Since the NaCN solutions were adjusted to pH > 12 using NaOH, a catalyst sample was treated with a NaOH aqueous solution as a control. Approximately 0.16 g of the original, thermally-pretreated Au/Al_2O_3 catalyst was contacted with 6 mL distilled, deionized H_2O adjusted to pH > 12 with a few drops of 1 M NaOH solution. After stirring for 70 min, the slurry was filtered and the catalyst was then re-suspended in 6 mL distilled, deionized H_2O for 15 min. This procedure was repeated prior to drying the catalyst in air at 310 K for 24 h.

2.3. X-ray absorption spectroscopy

The X-ray absorption spectra at the Au L_{III} edge were recorded on beam line X-10C at he National Synchrotron Light Source, Brookhaven National Laboratory, Upton, NY. The storage ring operated at 2.8 GeV with currents ranging from 150 to 300 mA. Several Au reference compounds, Au_2O_3, $AuCl_3$, and AuCl (all from Alfa Aesar, 99.99%), were diluted in BN powder (Alfa Aesar, 99.5%) and pressed into self-supporting wafers. Also, a light-tight Au foil (0.005 mm thick, Goodfellow, 99.9%) was used to drive Au–Au phase shift and amplitude functions. The spectra of the reference compounds and Au foil were collected in the transmission mode in air at ambient temperature. The spectra of the catalyst samples were collected in the fluorescence mode in a cell capable of heating and cooling the samples in a controlled atmosphere. Four scans were used for structural determination. Data analysis was performed with the WinXAS software package [19].

2.4. Reactor system

Kinetic data were collected with a fixed bed, quartz tubular reactor flow system operating at temperatures from ambient to 373 K and at ambient pressure. Between 5 and 100 mg of catalyst was diluted with 350–450 mg SiC (Universal Photonics, Inc., 120 mesh) to reduce axial gradients and by-passing.

Helium (BOC, 99.999%) was purified with a Supelco OMI-2 purifier and a silica gel (Davisil Grade 635 Type

60A, 60–100 mesh) trap at dry ice–acetone temperature. Dihydrogen (BOC, 99.999%) was purified with a Supelco OMI-2 purifier; CO (Messer, 99.997%) and O_2 (BOC, 99.999%) were each purified with silica gel traps at dry ice–acetone temperature.

Total volumetric gas flows of 75–250 mL min^{-1} were used. For CO oxidation studies, feed compositions of 0.3–7.0 mole% CO and O_2, up to 1.8 mole% H_2O, and balance He were used. For selective oxidation of CO in H_2, feed compositions of 0.3–3.5 mole% CO and O_2, up to 1.8 mole% H_2O, approximately 40 mole% H_2, and balance He were used. The reactor effluent was analyzed for CO, CO_2, O_2, and H_2O using gas chromatography. Prior to the collection of kinetic data, all samples were first pretreated *in situ* in 20 mL min^{-1} He at 623 K for 4 h.

3. Results and discussion

The Au loadings were 1.16, 0.24, and 0.16 wt.% for the original, 1 wt.% and 2 wt.% NaCN treated samples, respectively, as reported by Galbraith Laboratories, Inc. (Knoxville, TN). Analysis of the Au loading on the NaOH treated control sample was not performed; the Au loading was assumed to be the same as the original sample.

The Au oxidation state of the catalysts was determined using XAS. Figure 1 presents the X-ray absorption near-edge structure (XANES) of reference compounds having Au in various formal oxidation states. As shown in the figure, Au^{3+} compounds such as Au_2O_3 and $AuCl_3$ exhibit a large threshold absorption peak at the L_{III} edge. A smaller threshold peak is observed for a Au^{1+} compound, such as AuCl. For zero-valent Au foil, only a shoulder is observed at the L_{III} edge.

Figure 1 also shows the evolution of the original catalyst XANES with increasing pretreatment temperature in He. At ambient temperature, the Au appeared to be in a +3 oxidation state since a large threshold peak is present in the spectrum. As the temperature of the sample increased from 298 to 623 K, the threshold peak decreased in intensity, indicating autoreduction of the supported Au in flowing He. At 623 K, essentially all of the Au was reduced to the metallic state. No significant change in the catalyst XANES was observed during selective oxidation of CO in H_2 at 373 K following pretreatment in He at 623 K.

The extended X-ray absorption fine structure (EXAFS) of the reduced samples was used to characterize the atomic structure of the Au. The structural parameters, Au–Au coordination number (N), interatomic distance ($R_{Au–Au}$), and change in Debye–Waller factor compared to Au foil ($\Delta\sigma^2$) were obtained by curve-fitting the first-shell EXAFS data in both R space and k space. The average Au particle diameters (d_{Ave}) were

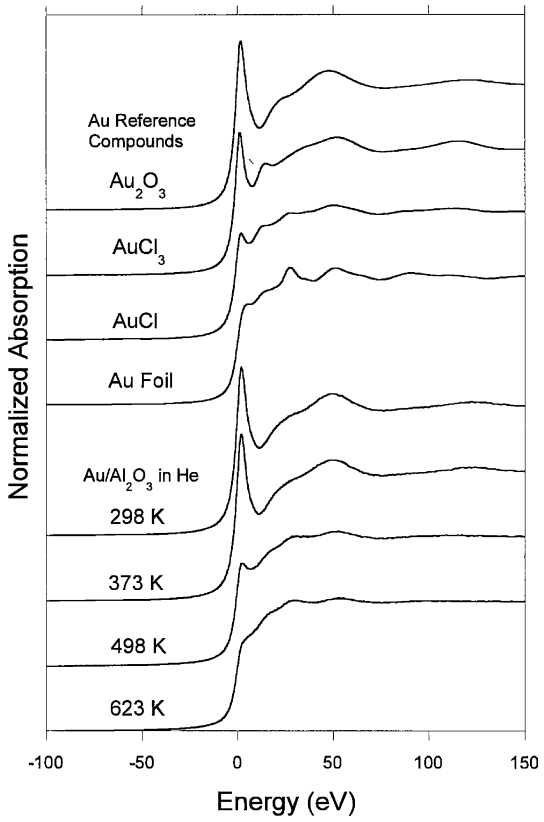

Figure 1. X-ray absorption near edge spectra at the Au L_{III} edge of Au reference compound and the original Au/Al_2O_3 catalyst during thermal pretreatment in He. Spectra are offset for clarity. The energies are defined relative to the first inflection point in the L_{III} edge of Au foil.

approximated from the first-shell coordination number assuming a spherical geometry [20].

The EXAFS of the original Au/Al_2O_3 sample in He after thermal treatment was recorded at ambient temperature [21]. The calculated values of N, $R_{Au–Au}$, $\Delta\sigma^2$, and d_{Ave}, are summarized in table 1. The structural parameters obtained from the catalyst EXAFS indicate a very high dispersion of Au on the support. For the original sample, the coordination number and interatomic distance were significantly smaller than the bulk gold values of 12 and 2.88 Å, respectively. In addition, the positive change in Debye–Waller factor compared to Au foil indicates greater thermal disorder, which is typical of highly dispersed metal particles.

The near edge spectra of the 2 wt.% NaCN treated sample in He at ambient temperature and 623 K are

Table 1
Au First Shell Structural Parameters

Sample	N (Au–Au)	R_{Au}(Å)	$\Delta\sigma^2$ (Å^2)	d_{Ave} (nm)
Original[a]	7.2	2.81	0.0031	1.2
2 wt.% NaCN	8.6	2.86	−0.0002	1.5

[a] From reference [21].

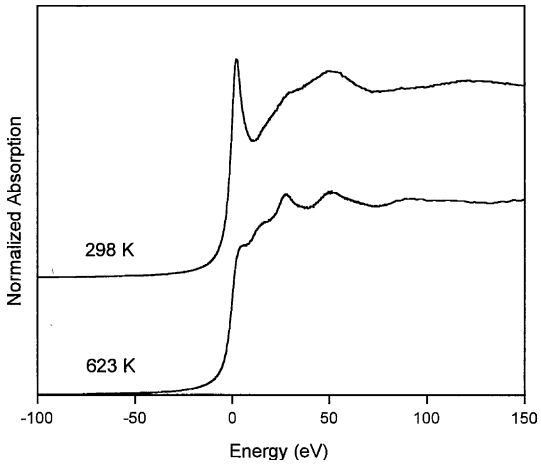

Figure 2. X-ray absorption near edge spectra at the Au L_{III} edge of the 2% NaCN treated Au/Al_2O_3 catalyst during thermal pretreatment in He. Spectra are offset for clarity. The energies are defined relative to the first inflection point in the L_{III} edge of Au foil.

shown in figure 2. Following the NaCN treatment, the sample at 298 K in He contained cationic Au, but autoreduction of the Au to a predominantly metallic state was observed during treatment at 623 K in He. The EXAFS function of the sample reduced at 623 K in He, the Fourier transform, and the Fourier-filtered first-shell contribution to the EXAFS function are presented in figure 3. The results from curve-fitting the experimental data are shown in figure 3(b) and (c). The calculated values of N, R_{Au-Au}, $\Delta\sigma^2$, and d_{Ave} are also presented in table 1. The structural parameters for the 2 wt.% NaCN treated sample suggest it contains slightly larger particles (1.5 nm) than the original sample (1.2 nm). Therefore, the NaCN treatment may have selectively leached smaller Au particles. Nevertheless, the catalysts in this study had a majority of Au metal atoms exposed.

A comparison of the kinetic results for the NaCN treated, NaOH treated, and original samples in the oxidation of CO and the selective oxidation of CO in H_2 can be found in tables 2 and 3, respectively. For CO oxidation, the rate of CO_2 formation per mole Au

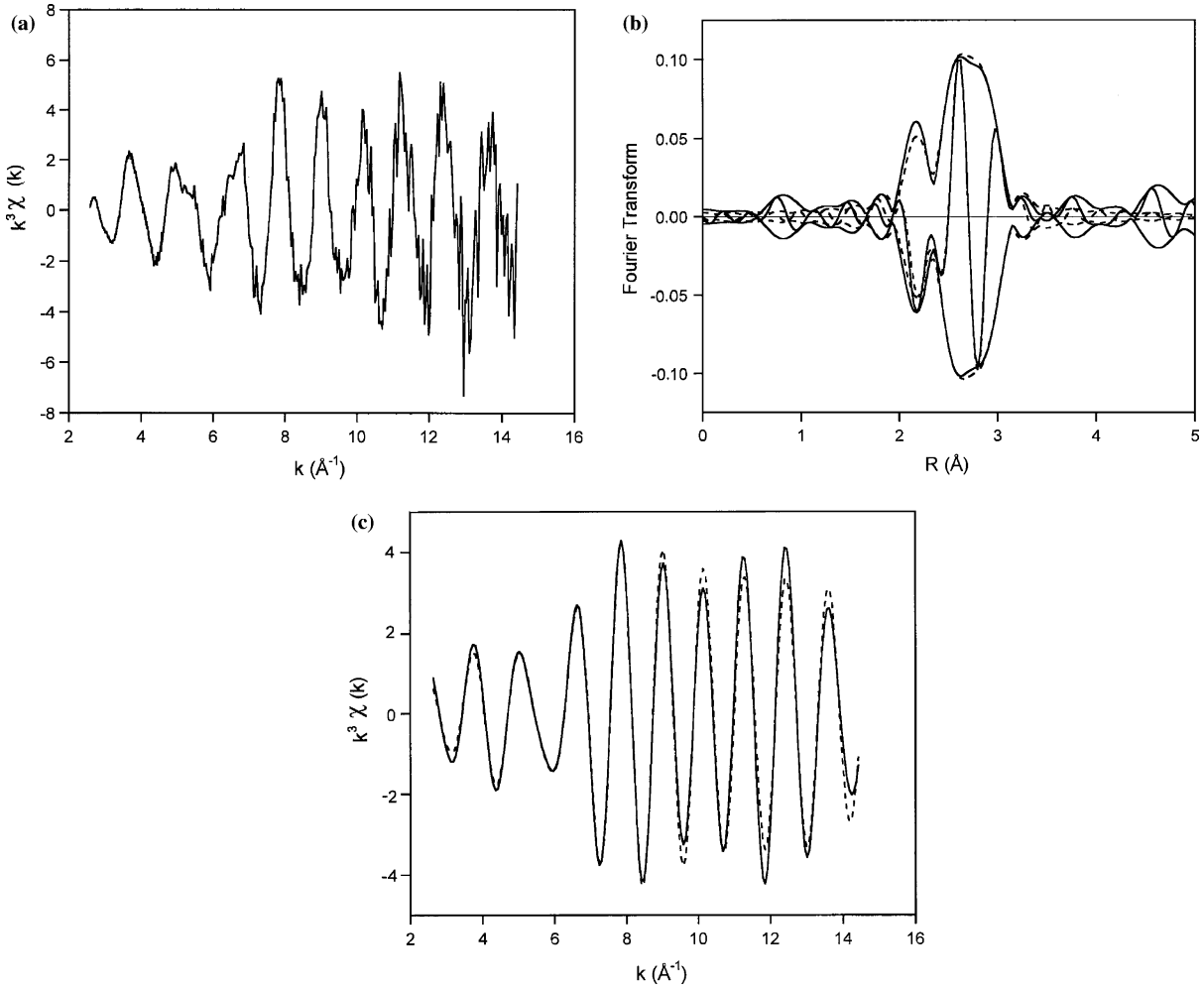

Figure 3. Extended X-ray absorption fine structure above the Au L_{III} edge of the 2 wt.% NaCN treated Au/Al_2O_3 catalyst in He at room temperature after pretreatment in He at 623 K. (a) Experimental $k^3\chi(k)$ data; (b) The magnitude and imaginary component of the Fourier transform, (uncorrected for phase shift) of $k^3\chi(k)$ from 2.6 to 14.5 $Å^{-1}$; results from the first shell curve fit are plotted as the dashed line; and (c) Comparison fitted EXAFS function (dashed line) to back transform (solid line) of first shell radial structure function from 1.9 to 3.4 Å.

Table 2
Kinetic results for CO oxidation

Sample	Au loading (wt.%)	Reaction rate (mol CO_2 (mol Au)$^{-1}$ s^{-1})		Activation energy[a] (kJ mol^{-1})	Orders of reaction[b]	
		298 K	373 K		O_2	CO
Original	1.16	0.014	0.036	12	0.36	0.32
NaOH	1.16[c]	0.017	0.062	16	0.29	0.30
1 wt.% NaCN	0.24	0.015	0.083	20	0.34	0.28
2 wt.%NaCN	0.16	0.016	0.072	18	0.40	0.39

[a] 95% CI ± 1 kJ mol^{-1}.
[b] Determined at ambient temperature; 95% CI ± 0.04.
[c] Not determined, assumed to be the some as the original catalyst loading.

Table 3
Kinetic results for selective oxidation of CO in H_2

Sample	Au loading (wt.%)	Reaction rate (mol CO_2 (mol Au)$^{-1}$ s^{-1}) 298 K	Orders of Reaction[a]		Selectivity[b] 373 K
			O_2	CO	
Original	1.16	0.092	0.33	0.09	40–45%
NaOH	1.16[c]	0.058	0.34	0.09	37%
1 wt.% NaCN	0.24	0.115	0.35	0.06	50–55%
2 wt.%NaCN	0.16	0.059	0.31	0.03	55–60%[a]

[a] Determined at ambient temperature; 95% CI ± 0.04.
[b] Conversion ranged from 50–85% at 373 K. Water content at 298 K was below detection limit.
[c] Not determined, assumed to be the same as the original catalyst loading.

(0.015 ± 0.002 s^{-1} at 298 K), apparent activation energy (16 ± 4 kJ mol^{-1}), and orders of reaction with respect to O_2 (0.34 ± 0.06) and CO (0.34 ± 0.06) were relatively unaffected by the NaCN treatment. However, some differences were observed for the selective oxidation of CO in H_2. The rates of reaction at 298 K were accelerated over all of the catalysts by the presence of H_2. During selective oxidation of CO in H_2, H_2O is produced via H_2 oxidation. The selectivity of CO oxidation over H_2 oxidation at 373 K is reported in table 3. The low water content in the product stream prevented the calculation of the selectivity at 298 K. The normalized rates at 298 K varied among the catalysts by about a factor of 2. The lack of consistency among the rates was likely due to the small, unquantifiable variation in water produced by oxidation of H_2 at 298 K. The order of reaction in O_2 was unaffected by H_2, but the order with respect to CO decreased significantly (see tables 2 and 3).

Haruta and co-workers examined the effect of co-fed H_2O on the rate of CO oxidation in over Au supported on TiO_2 [22]. They observed a significant promotional effect on the rate of reaction when performed in the presence of H_2O. A similar promotional effect was observed on the rate of reaction with Au/Al_2O_3 catalysts at ambient temperature as shown in figure 4. The presence of H_2O increased the rate of CO oxidation to a greater extent for the NaCN treated samples compared to the original and NaOH treated samples.

The NaCN treatment and thermal procedure applied to Au/Al_2O_3 resulted in a different evolution in the Au oxidation state compared to previously published results with Au supported on $Ce(La)O_2$. As described earlier, cationic Au was stabilized at defects on $Ce(La)O_2$ and was shown to contribute to the water–gas shift activity of the catalysts [17]. In the current work, the original Au/Al_2O_3 prior to thermal treatment in He at 623 K contained predominately Au^{3+}, whereas after thermal

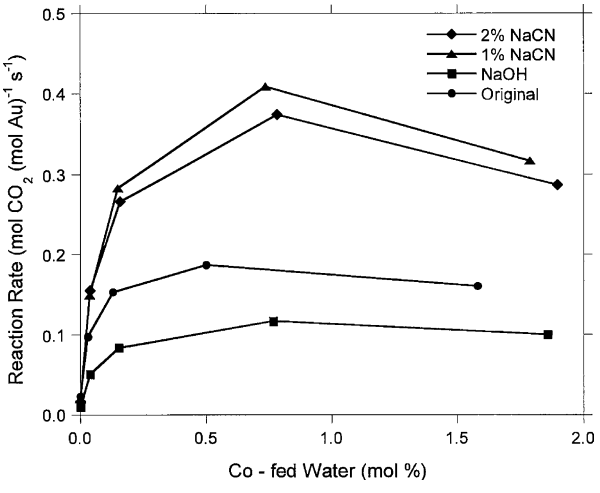

Figure 4. Effect of co-fed water on the rate of CO oxidation at 298 K.

treatment it contained predominately Au° (figure 1). Likewise, a reduced sample treated with NaCN contained cationic Au, but was also reduced to metallic Au after a second thermal treatment. Since the reaction rate for CO oxidation was proportional to the metallic Au in the sample, it appears that metallic Au is required for the reaction. However, the fraction of Au that participates in the reaction is quite low. Using isotopic transient analysis to characterize the original Au/Al_2O_3 used in this study, we found the surface coverage of carbon-containing reactive species to be approximately 5% [21]. Also, Oh *et al*. [23] found that a Cl/Au molar ratio of 0.006 reduced activity, which also indicates the fraction of active Au is very low. Since a small fraction of cationic Au could remain undetected by XAS, the current work does not eliminate the possibility of cationic Au being present in active Au/Al_2O_3 catalysts for CO oxidation. However, the available evidence suggests an important role of zero-valent Au.

4. Conclusions

Treatment of Au/Al_2O_3 with 2 wt.% NaCN solution removed nearly 90% of the Au. For the oxidation of CO in a dry atmosphere, the rate correlated directly to the Au loading, thus, giving a constant turnover frequency for the reaction. In addition, the apparent activation energy and the orders of reaction were not affected by the removal of Au by NaCN treatment. The rate was accelerated by the presence of H_2 and H_2O over all of the catalysts. Interestingly, different kinetic behavior was observed over the samples when the reaction was performed in the presence of H_2O. The variability of activity with H_2O is likely the cause of wide range of results in the literature for similar catalyst preparations. Thermal treatment of the original Au/Al_2O_3 catalyst caused reduction of the Au into 1.2 nm sized metal particles, as evaluated by XAS. Although treatment with NaCN solution removed most of the Au and left cationic Au on the support, subsequent thermal treatment reduced the remaining Au to metal particles of about 1.5 nm in diameter. The interaction of Au on alumina was not strong enough to preserve its cationic state under moderate temperature, and metallic Au appeared to be important for the CO oxidation reaction.

Acknowledgments

This work was supported by the National Science Foundation (Grant # CTS-0121619). Research was carried out in part at the National Synchrotron Light Source, Brookhaven National Laboratory, which is supported by the U.S. Department of Energy, Division of Materials Sciences and Division of Chemical Sciences, under Contract No. DE-AC02 98CH10886. We thank M. Flytzani-Stephanopoulos for the details of the NaCN treatment.

References

[1] B. Hammer and J.K. Norskov, Nature 376 (1995) 238.
[2] M. Haruta, N. Yamada, T. Kobayashi and S. Iijima, J. Catal. 115 (1989) 301.
[3] R.J. Davis, Science 301 (2003) 926.
[4] L.D. Socaciu, J. Hagen, T.M. Bernhardt, L. Woste, U. Heiz, H. Hakkinen and U. Landman, J. Am. Chem. Soc. 125 (2003) 10437.
[5] A. Sanchez, S. Abbet, U. Heiz, W.-D. Schneider, H. Hakkinen, R.N. Barnett and U. Landman, J. Phys. Chem. A 103 (1999) 9573.
[6] H. Hakkinen, S. Abbet, A. Sanchez, U. Heiz and U. Landman, Angew. Chem. Int. Ed. 42 (2003) 1297.
[7] M. Okumura, S. Nakamura, S. Tsubota, T. Nakamura, M. Azuma and M. Haruta, Catal. Lett. 51 (1998) 53.
[8] M. Okumura, S. Tsubota and M. Haruta, J. Mol. Catal. A: Chem. 3949 (2003) 1.
[9] N. Lopez, T.V.W. Janssens, B.S. Clausen, Y. Xu, M. Mavrikakis, T. Bligaard and J.K. Norskov, J. Catal. 223 (2004) 232.
[10] Z.-P. Liu, P. Hu and A. Alavi, J. Am. Chem. Soc. 124 (2002) 14770.
[11] M. Valden, X. Lai and D.W. Goodman, Science 281 (1998) 1647.
[12] J. Guzman and B.C. Gates, J. Phys. Chem. B 106 (2002) 7659.
[13] N.A. Hodge, C.J. Kiely, R. Whyman, M.R.H. Siddiqui, G.J. Hutchings, Q.A. Pankhurst, F.E. Wagner, R.R. Rajaram and S.E. Golunski, Catal. Today 72 (2002) 133.
[14] G.C. Bond and D.T. Thompson, *Gold Bull*. 33(2) (2000) 41.
[15] C.K. Costello, M.C. Kung, H.-S. Oh, Y. Wang and H.H. Kung, Appl. Catal. A: Gen. 232 (2002) 159.
[16] H.S. Oh, C.K. Costello, C. Cheung, H.H. Kung and M.C. Kung, Stud. Surf. Sci. Catal. 139 (2001) 375.
[17] Q. Fu, H. Saltsburg and M. Flytzani-Stephanopoulos, Science 301 (2003) 935.
[18] H.H. Kung, M.C. Kung and C.K. Costello, J. Catal. 216 (2003) 425.
[19] T. Ressler, WinXAS version 2.33 (1992–2002).
[20] R.B. Greegor and F.W. Lytle, J. Catal. 63 (1980) 476.
[21] J.T. Calla and R.J. Davis, J. Phys. Chem. B. In press.
[22] M. Date and M. Haruta, J. Catal. 201 (2001) 221.
[23] H.-S. Oh, J.H. Yang, C.K. Costello, Y.M. Wang, S.R. Bare, H.H. Kung and M.C. Kung, J. Catal. 210 (2002) 375.